Thermodynamic properties and magnetic excitations in MnTe systems

1997 J. Phys.: Condens. Matter 9 6901

(http://iopscience.iop.org/0953-8984/9/32/012)

J. Phys.: Condens. Matter **9** (1997) 6901–6912. Printed in the UK PII: S0953-8984(97)82172-8

Thermodynamic properties and magnetic excitations in MnTe systems

R Świrkowicz†
Institute of Physics, Warsaw University of Technology, Koszykowa 75, 00-662 Warsaw, Poland

Received 26 February 1997, in final form 12 June 1997

Abstract. MnTe systems with fcc structure and long-range antiferromagnetic ordering of type III is investigated within the framework of the Heisenberg model. The Hamiltonian includes exchange interactions with the nearest and the next-nearest neighbours, anisotropy and Zeeman terms. Calculations are performed using the Green's function formalism. Temperature dependencies of the spin-wave energy and the integrated intensity of the Stokes peak are determined. The calculated curves are consistent with the results obtained for bulk-like MnTe films with the use of the Raman spectroscopy.

1. Introduction

It has been experimentally established that CdMnTe and ZnMnTe compounds with zinc blende (ZB) crystallographic structures reveal long-range antiferromagnetic ordering when the concentration of Mn is relatively high. Detailed investigations performed with the use of the neutron diffraction show that the antiferromagnetic phase of type III appears for concentrations as high as 0.8 [1]. It should be pointed out that samples with ZB structures and such high concentrations of Mn can only be produced by the MBE technique [2]. However, fabricated single-crystal epilayers of MnTe, ZnMnTe or CdMnTe compounds can be several micrometres thick, so in fact such films show bulk properties.

According to [1] MnTe films and compounds with very high Mn concentration represent typical Heisenberg systems with a very small anisotropy field as compared with the exchange field. The nearest- as well as the next-nearest-neighbour spins couple antiferromagnetically and lead to the AFM-III phase. The systems are strongly frustrated. Neutron diffraction studies reveal a presence of three types of domain configurations in which AF sheets are perpendicular to the appropriate crystalline axis. While in a bulk system all such states are equivalent, in epitaxial layers there is a kind of asymmetry resulting from stress effects. Detailed measurements performed in [1] show that, in the case of strained MnTe layers, as well as for compounds with Mn concentration slightly lower than 1, the temperature dependence of the reduced magnetization corresponds closely to the Brillouin function over the whole temperature region. However, for pure MnTe bulk-like films a much sharper fall of the magnetization is observed, but only in the close vicinity of the experimentally established Néel temperature. This temperature is lower than that corresponding to the Brillouin dependence.

Raman spectra taken for MnTe epilayers, as well as for MBE grown layers with high Mn concentration, reveal a presence of a peak corresponding to the one-magnon scattering

† E-mail address: renatas@if.pw.edu.pl

0953-8984/97/326901+12$19.50

[3, 4]. Magnon peaks, however, with essentially lower energies, were observed in Raman spectra of bulk mixed CdMnTe crystals with relatively high Mn concentrations (between 0.4 and 0.7) [5]. Magnons in bulk mixed crystals were also investigated with the use of the neutron-scattering technique, and dispersion relations for modes which propagate in two different directions were found [6]. The obtained results were compared with those found theoretically for diluted systems using computer-simulation methods [7, 8].

Magnons in antiferromagnetic MnTe bulk systems and in ultrathin films were studied very recently [9]. The investigations have been performed for zero temperature within the framework of the spin-wave approach.

In recent years there has been an increasing interest in the studies of MnTe systems. It was stimulated by experimental investigations performed for bulk-like MBE-grown epilayers. However, despite many experimental papers only a few tackle the theoretical approach to the problem, especially when temperatures above zero are considered. Up to now, attempts mainly based on the simple molecular-field theory were used for explanation of thermodynamic properties of bulk mixed crystals. The region of low Mn concentration only was investigated.

It appears that more extended theoretical investigations performed for MnTe systems are required. The aim of the present paper is to study some thermodynamic properties of MnTe antiferromagnets with ZB structure. Raman-scattering processes due to magnons in such systems will also be investigated. All calculations are performed in a uniform and self-consistent way using the Green's function formalism. Comparison of the results with experimental data, obtained with the use of various techniques, allows us to describe the MnTe compounds in a more homogeneous way.

2. Green's function formalism: thermodynamic properties of MnTe systems

Neutron diffraction studies clearly show that magnetic ordering in MnTe compounds corresponds to AFM of type III [1]. Such systems can be described by taking into account two equivalent magnetic sublattices [9, 10]. The Heisenberg Hamiltonian can, therefore, be written in the form

$$H = \tfrac{1}{2}\sum_{ll'} J_{ll'}\underline{S}_l\underline{S}_{l'} + \tfrac{1}{2}\sum_{LL'} J_{LL'}\underline{S}_L\underline{S}_{L'} + \sum_{lL} J_{lL'}\underline{S}_l\underline{S}_L - \mathcal{H}_A\left(\sum_l S_l^z - \sum_L S_L^z\right) - \mathcal{H}_0\left(\sum_l S_l^z + \sum_L S_L^z\right) \tag{1}$$

where indices l and L correspond to sublattices 1 and 2, respectively and $\mathcal{H}_A$, $\mathcal{H}_0$ represent anisotropy and external fields expressed in $g\mu_B$ units. It means that $\mathcal{H}_0 = g\mu_B H_0$ in the case when the external magnetic field H_0 is applied along the z-axis. In MnTe compounds the nearest- and the next-nearest-neighbour exchange interactions should be taken [6]. The appropriate integrals will be denoted by J_1 and J_2. Neutron diffraction measurements performed for CdMnTe crystals with a high concentration of Mn ($x \approx 0.7$) as well as measurements performed for systems with very low Mn concentration ($x < 0.05$) show that J_1 is much greater than J_2 [6, 11, 12].

Green's functions $\langle\langle S_i^+, S_j^-\rangle\rangle$ which satisfy the equation of motion

$$E\langle\langle S_i^+, S_j^-\rangle\rangle = \frac{1}{2\pi}\langle[S_i^+, S_j^-]\rangle + \langle\langle[S_i^+, H], S_j^-\rangle\rangle \tag{2}$$

can be introduced. The indices i, j correspond to both sublattices. When the standard RPA

decoupling is used Fourier transforms of $\langle\langle S_i^+, S_j^-\rangle\rangle$ take the following forms

$$G_{11}(k) = \frac{\langle S_1\rangle}{\pi}\frac{\{E - [\mathcal{H}_0 - \mathcal{H}_A - 2J(\langle S_1\rangle + \langle S_2\rangle) + 2J_k\langle S_2\rangle]\}}{(E - E_k^+)(E - E_k^-)} \tag{3}$$

$$G_{22}(k) = \frac{\langle S_2\rangle}{\pi}\frac{\{E - [\mathcal{H}_0 + \mathcal{H}_A - 2J(\langle S_1\rangle + \langle S_2\rangle) + 2J_k\langle S_1\rangle]\}}{(E - E_k^+)(E - E_k^-)} \tag{4}$$

$$G_{21}(k) = \frac{1}{\pi}\frac{\langle S_1\rangle\langle S_2\rangle J_{12}(k)}{(E - E_k^+)(E - E_k^-)} \tag{5}$$

where $G_{11}(k)$ corresponds to the Fourier transform of $\langle\langle S_l^+, S_l^-\rangle\rangle$, $G_{22}(k)$ corresponds to the transform of $\langle\langle S_L^+, S_L^-\rangle\rangle$ and $\langle S_1\rangle$ and $\langle S_2\rangle$ represent the mean magnetic moments in both sublattices. In the presence of the external magnetic field H_0 the quantities can be expressed as follows: $\langle S_1\rangle = \langle S\rangle + \chi_\parallel H_0$, $\langle S_2\rangle = -\langle S\rangle + \chi_\parallel H_0$, where $\chi_\parallel$ is the magnetic susceptibility parallel to the field H_0. In formulae (3)–(5) E_k^+, E_k^- correspond to the spin-wave energies. For the system under consideration the energies are given by

$$E_k^\pm = [\mathcal{H}_0 - 2H_0\chi_\parallel(2J - J_k)] \pm \{[\mathcal{H}_A + 2J_k\langle S\rangle]^2 - \langle S\rangle^2 J_{12}^2(k) + \chi_\parallel^2 H_0^2 J_{12}^2(k)\}^{1/2} \tag{6}$$

where

$$J = 4J_1 + J_2 \tag{7}$$

$$J_k = 2J_1 - J_2 + J_1\left(\cos\frac{k_x a}{2}\cos\frac{k_y a}{2} + \cos\frac{k_z a}{2}\cos\frac{k_y a}{2}\right) + J_2(\cos k_x a + \cos k_z a) \tag{8}$$

$$J_{12}(k) = 2J_1\left(2\cos\frac{k_x a}{2}\cos\frac{k_z a}{2} + \cos\frac{k_x a}{2}\cos\frac{k_y a}{2} + \cos\frac{k_z a}{2}\cos\frac{k_y a}{2}\right) + 2J_2\cos k_y a. \tag{9}$$

In the absence of the magnetic field for $k = 0$ one obtains the standard expression for the spin-wave energy in an antiferromagnetic medium, namely

$$E_0 = \{\omega_A(\omega_A + 2\omega_E)\}^{1/2} \tag{10}$$

where $\omega_A = \mathcal{H}_A$ is the anisotropy energy and $\omega_E = 2J\langle S\rangle$ represents the exchange energy in the case of MnTe.

Within the Green's function formalism the spin-wave energy depends on the sublattice magnetization $\langle S\rangle$. The temperature dependence of the magnetization can be calculated in a consistent way when the approach presented in [13, 14] is used. For general spin S one can write

$$\langle S\rangle = \frac{2S+1}{2}\left[\frac{(x+1)^{2S+1} + (x-1)^{2s+1}}{(x+1)^{2S+1} - (x-1)^{2S+1}}\right] - \frac{x}{2} \tag{11}$$

where

$$x = \frac{1}{N}\sum_k \frac{\mathcal{H}_A + 2J_k\langle S\rangle}{E_k}\,\mathrm{cth}\,\frac{E_k}{2k_B T} \tag{12}$$

with E_k equal to E_k^+ in equation (6) for the case $H_0 = 0$. To calculate $\langle S(T)\rangle$ using formulae (11) and (12) the temperature dependence of the anisotropy energy should be determined first. In the general case the origin of the anisotropy should be discussed. However, it is not the main problem to be discussed here. Moreover, experimental investigations clearly show that the anisotropy in MnTe systems is very small as compared with the exchange energy (see, e.g. [1, 6]) and in all relations in which the exchange plays an important role, the anisotropy energy can be estimated in an approximate way. It seems to be reasonable to assume the relation: $\mathcal{H}_A(T) = K_A\frac{\langle S\rangle}{S}$, where K_A is the temperature independent constant.

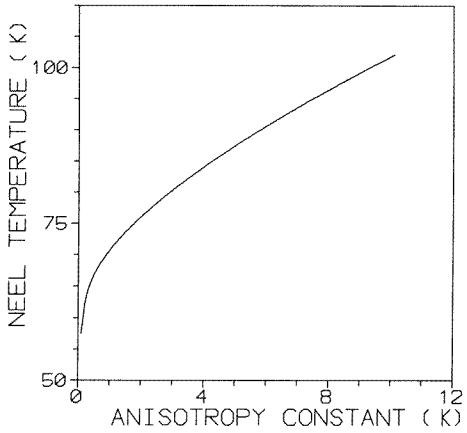

Figure 1. The Néel temperature of the MnTe system versus anisotropy constant K_A.

The Néel temperature within the Green's function formalism can be calculated according to the formula [14]

$$T_N = \frac{S(S+1)}{3k_B}\left[\frac{1}{N}\sum_k \frac{K_A/S + 2J_k}{(K_A/S + 2J_k)^2 - J_{12}^2(k)}\right]^{-1}. \tag{13}$$

Figure 1 presents the dependence of T_N on anisotropy parameter K_A. Integrals J_1 and J_2 are taken from neutron diffraction measurements [6]. Calculations are performed for $J_1 = 13.4$ K and $J_2 = 0.1J_1$. On the other hand, K_A strongly influences spin-wave energy for the wavevector $k = 0$ (equation (10)). Estimation of K_A from the magnon energy measured in the Raman scattering at low temperatures [15] leads to an anisotropy constant equal to 5.65 K. The Néel temperature obtained for this value of K_A is equal to 89.5 K (figure 1). The exchange integral J_2 cannot be determined from the neutron diffraction measurements with high precision (see [6]). Therefore, we tested the influence of J_2 on T_N. The results presented in figure 2 show that, for a given anisotropy constant, values of J_2 close to $0.1J_1$ (as suggested by experimental data [6]) correspond to the maximum of T_N.

Neutron diffraction studies performed on bulk-like MnTe films show that, at relatively low temperatures, experimental data for the magnetization closely follow the Brillouin function corresponding to a Néel temperature equal to 88 K [1] which is consistent with the result obtained in this paper. However, it should be pointed out that, in pure unstrained MnTe films, the character of the temperature dependence of the magnetization changes around $T = 60$ K and the abrupt disappearance of magnetization is observed which probably corresponds to the changes in the type of the phase transition [1]. Such a behaviour of the real system certainly cannot be described within the framework of the formalism used in the paper.

When magnon–magnon interactions are not taken into account, temperature dependence of the spin-wave energy E_0 given by equation (10) is in fact determined by $\langle S(T)\rangle$. It is depicted in figure 3 for the values of the parameters given above. The values of energy corresponding to magnon peaks at various temperatures in Raman spectra of bulk-like MnTe films are also presented in the figure (after [15]). A good consistency between experimental and theoretical results can be observed.

Next, the temperature dependence of the magnetic susceptibility is found. Calculations

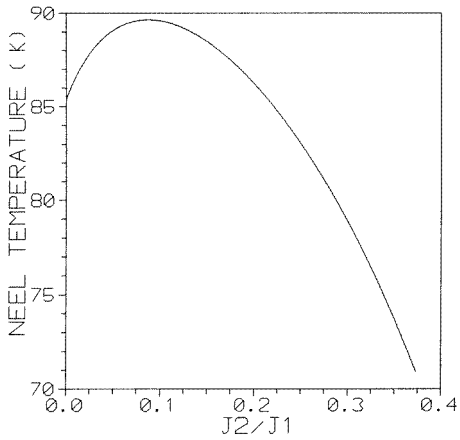

Figure 2. The Néel temperature of the MnTe system versus the J_2/J_1 ratio. The curve corresponds to K_A estimated according to Raman scattering [15].

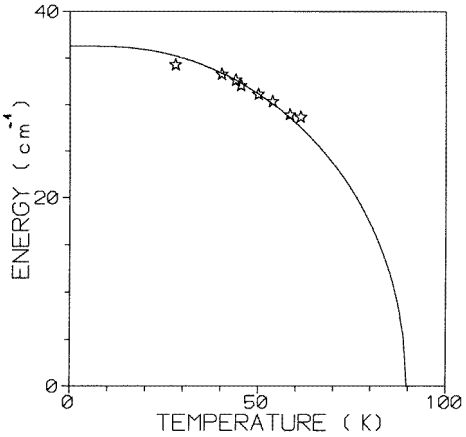

Figure 3. The temperature dependence of the spin-wave energy. The points correspond to experimental data obtained from Raman scattering in [15].

are performed within the framework of the Green's function formalism (see [14]). Results obtained for $\chi_\parallel$ are presented in figure 4. For $T = T_N$ the susceptibility χ is equal to $g\mu_B/4J$ as in a molecular-field approach.

Temperature dependence of the magnetic susceptibility was investigated experimentally for the case of bulk-like MnTe films [16]. In fact no essential difference between $\chi_\perp$ and $\chi_\parallel$ was seen. It is very probable that such a result is a consequence of the fact that real systems are strongly frustrated. The domains with AF sheets perpendicular to three cubic axes can be present in MnTe according to neutron diffraction studies [1, 6]. In such a situation it would be reasonable to introduce the average susceptibility χ_{av} instead of $\chi_\parallel$ and $\chi_\perp$ as in typical AF systems. In figure 5 temperature dependencies of the spin-wave modes $E_0^\pm$ resulting from (6) for $k = 0$ are given. The curves calculated with the use of $\chi_\parallel$ obtained for the typical AF state and with the use of χ_{av} are presented. For very low temperatures the splitting of the modes is significantly smaller with χ_{av} used. When the external field

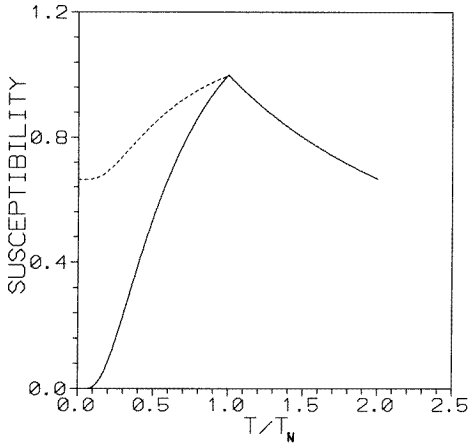

Figure 4. The temperature dependence of the parallel susceptibility $\chi_{\parallel}$ calculated for antiferromagnetic MnTe. The broken curve corresponds to χ_{av}.

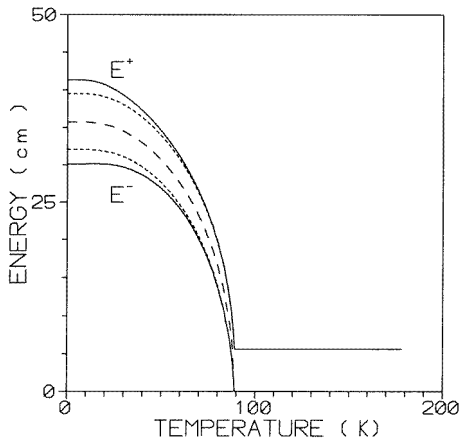

Figure 5. The temperature dependence of spin-wave E^+ and $|E^-|$ modes in the presence of $H_0 = 6T$. Full curves correspond to E^+ and $|E^-|$ calculated with $\chi_{\parallel}$ taken into account. Short broken curves are the calculations made with χ_{av} taken into account. The mode obtained for $H_0 = 0$ is also given.

$H_0 = 6T$ is applied the separation ΔE of the two modes at $T = 0$ K is equal to 7.47 cm^{-1} with χ_{av} taken into account, whereas for $\chi_{\parallel} = 0$ one obtains $\Delta E = 11.2$ cm^{-1}. It should be pointed out that Raman scattering measurements in the presence of the magnetic field were performed for mixed CdMnTe bulk crystals with a high Mn concentration ($x \cong 0.7$) [5]. The separation between two spin-wave modes for $H_0 = 6T$ was found to be 7 cm^{-1}. The consistency is surprisingly good, so it is tempting to interpret the result as a consequence of the mechanism described above.

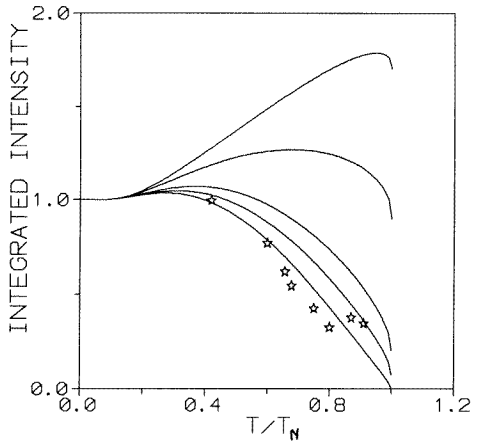

Figure 6. The temperature dependence of the integrated intensity for various values of the G/K ratio ($G/K = 0.0$, 0.01, 0.05, 0.10, 0.50 correspond to curves from the highest to the lowest value, respectively). Points are experimental data obtained from Raman scattering in [15].

3. One-magnon light scattering

A one-magnon light scattering cross section was investigated in many papers (see e.g. [17, 18]). For the system under consideration the integrated intensity corresponding to the Stokes peak in the case $H_0 = 0$ can be calculated according to the formula

$$\frac{\mathrm{d}h}{\mathrm{d}\Omega} \sim \frac{\langle S(T)\rangle}{E_0}\frac{1}{1-\exp(-E_0/k_BT)}\left\{\mathcal{H}_A^{1/2} + 2\frac{G}{K}p(T)\langle S(T)\rangle(\mathcal{H}_A + 4J\langle S(T)\rangle)^{1/2}\right\}^2 \qquad (14)$$

where K and G refer to the linear and quadratic magneto-optic coupling terms, respectively [17]. Only terms corresponding to in-phase scattering are taken into account [17]. Function $p(T)$ appears in the process of decoupling of higher-order Green's functions. According to Callen [19] it can be taken in the form $p(T) = 1 - 1/S^2[S(S+1) - \langle S^2\rangle]$.

The integrated scattering cross section was calculated for various values of G/K; the ratio is treated as a parameter. Obtained curves are given in figure 6. The influence of the quadratic coupling G on the Stokes scattered intensity appears to be rather strong. For $G/K = 0.05$ the intensity quite sharply decreases in the region of higher temperatures. According to formula (14) one can see that the influence of G is essentially enhanced by the exchange field, which is very strong in MnTe systems. Experimental points are also presented in the figure 6 (after [15]). The Raman data seem to fit the curve with $G/K = 0.5$ in the best way, though there are some discrepancies, especially in the region of the middle temperatures.

The integrated Raman intensity was calculated also for $H_0 \neq 0$. Results obtained for $G/K = 0.1$ are presented in figures 7(a) and (b). The different temperature dependence of the susceptibility is taken into account in both cases, namely the typical AF dependence for $\chi_\parallel$ (figure 7(a)) and $\chi_{\mathrm{av}}(T)$ relation which seems to fit experimental data more closely (figure 7(b)). The integrated intensity $\mathrm{d}h^+/\mathrm{d}\Omega$ (figures 7(a) and (b)) corresponds to the Stokes peak at $\hbar\omega_2 = \hbar\omega_1 - E_0^+$, whereas $\mathrm{d}h^-/\mathrm{d}\Omega$ corresponds to the Stokes peak at $\hbar\omega_2 = \hbar\omega_1 - |E_0^-|$. ω_1 and ω_2 are incident and scattered frequencies of light and E_0^+, E_0^- are magnon energies in the presence of the magnetic field for the wavevector $k = 0$. The total intensity $\mathrm{d}h/\mathrm{d}\Omega = \mathrm{d}h^+/\mathrm{d}\Omega + \mathrm{d}h^-/\mathrm{d}\Omega$ is also given. Intensities presented in figure 7

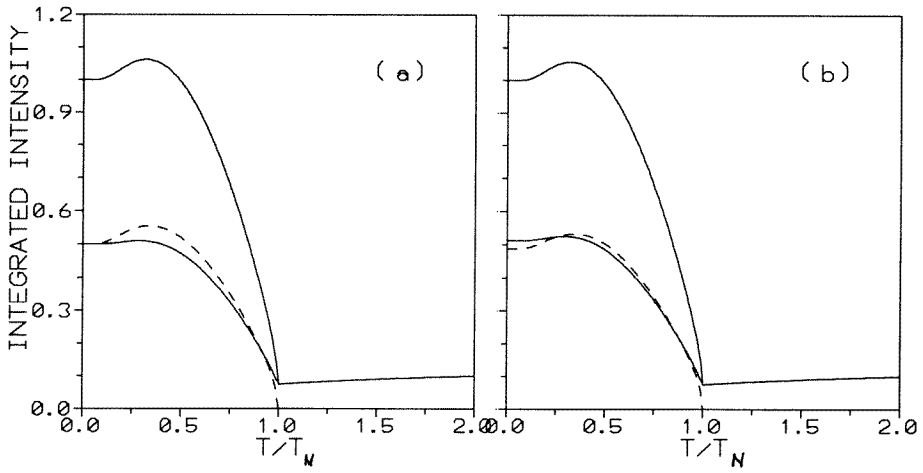

Figure 7. The temperature dependence of the integrated intensity in the presence of the field $H_0 = 6T$. Full curves correspond to $\mathrm{d}h^+/\mathrm{d}\Omega$ and $\mathrm{d}h^+/\mathrm{d}\Omega + \mathrm{d}h^-/\mathrm{d}\Omega$. The broken curve corresponds to $\mathrm{d}h^-/\mathrm{d}\Omega$ (see text). (*a*) is calculated with $\chi_\parallel$ and (*b*) is calculated with χ_{av}.

are normalized to the value obtained for $T = 0$ K. Because $\chi_{\mathrm{av}} \neq 0$ the asymmetry of the intensity $\mathrm{d}h^+/\mathrm{d}\Omega$ and $\mathrm{d}h^-/\mathrm{d}\Omega$ is obtained at low temperatures (figure 7(*b*)). Such an effect is not observed in the case of typical antiferromagnets with $\chi_\parallel(0) = 0$ (figure 7(*a*)). The comparison of the calculated results with experimental data for the integrated Raman intensity would be very interesting. However, at present the appropriate experimental results are not available.

4. Density of magnon states: two-magnon scattering

The dispersion relation of the spin-wave mode can be found according to equation (6) (for $H_0 = 0$). The curves obtained for different directions of propagation calculated with the use of the parameters taken above are presented in figure 8. It should be pointed out that the spin-wave energy strongly depends on the direction of propagation. The lowest energy corresponds to the case when the mode propagates in the direction perpendicular to the AF sheets ([010] direction in the case under consideration, see equation (6)). However, one can expect that in real systems because of a presence of domains with AF sheets perpendicular to three crystallographic axes the spin-wave energy can be averaged and independent of the direction of propagation along the cubic axes.

The density of magnon states is derived from the imaginary part of the Green's function. At zero temperature the following formula is used

$$g(E) = \frac{\langle S(0)\rangle}{N} \sum_k \frac{\{K_A/S + 2J_k - J_{12}(k)\}^{1/2}}{\{K_A/S + 2J_k + J_{12}(k)\}^{1/2}} \delta(E - E_k). \tag{15}$$

The curve calculated for the MnTe compound is given in figure 9. Two well pronounced peaks can be observed in the density of states. Energies close to the first one correspond to several points in the Brillouin zone mainly with k_x and k_y components different from zero. On the other hand, it is easy to check that the peak found at higher energies mainly corresponds to the L point at the Brillouin zone boundary with the wavevector

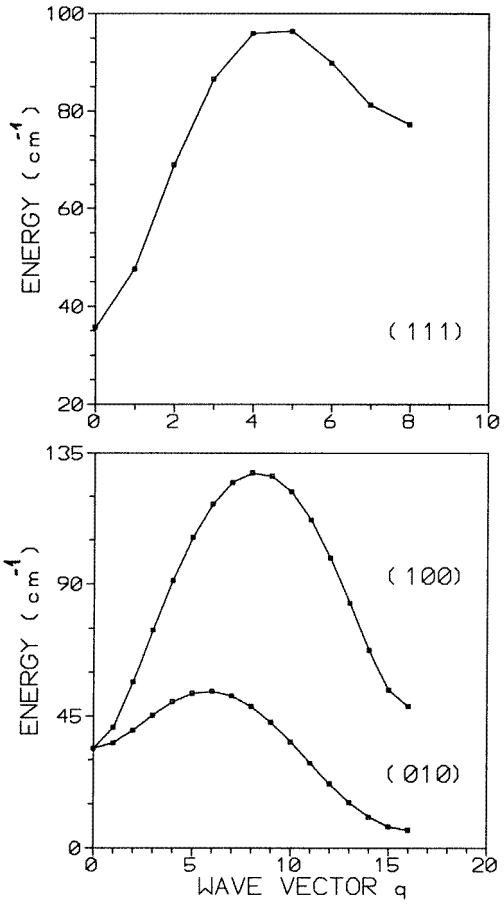

Figure 8. Spin-wave dispersion curves calculated for different propagation directions.

$\underline{k} = \frac{\pi}{a}(1, 1, 1)$. The question that now arises is: Can such states influence two-magnon scattering?

The intensity of two-magnon light scattering in simple antiferromagnetic systems can be assumed as proportional to the imaginary part of the Green's function $\langle\langle A, A^{+}\rangle\rangle$ with the operator A defined as [20, 21]

$$A = \sum_{j\delta} \phi_{\delta} \underline{S}_j \underline{S}_{j+\delta} \tag{16}$$

where ϕ_{δ} depends on the symmetry of the scattering mode and on the amplitude and polarization vectors of incident and scattered light. In the simple approximation at zero temperature when interactions between spin waves are not taken into account the following expression can be obtained for two-magnon Raman scattering intensity

$$I(E) \sim \frac{1}{N} \sum_{k} |\phi(k)|^2 \frac{(\mathcal{H}_A + 2J_k\langle S\rangle - J_{12}(k)\langle S\rangle)^2}{E_k^2} \delta(E - 2E_k) \tag{17}$$

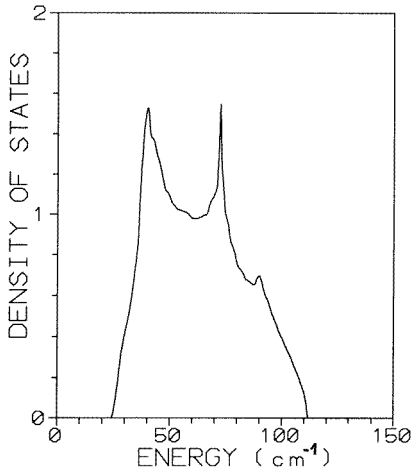

Figure 9. The density of magnon states.

where $\phi(k)$ corresponds to the Fourier transform of ϕ_δ. For xz geometry one has:

$$\phi(k) = 4 \sin \frac{ak_x}{2} \sin \frac{ak_z}{2}.$$

Two-magnon intensity, calculated according to formula (17), is presented in figure 10 for two different geometries. Some asymmetry can be seen. The shape of the peak according to the figure depends on the geometry. In the presented approach, with no magnon interactions taken into account, the main peak appears at the energy about 155 cm^{-1} for both polarizations. One can expect the shifting of the peak towards lower energies when the magnon–magnon interactions are taken into account [20]. Therefore, it is possible that the two-magnon peak can appear in MnTe systems in the range of energies 140–155 cm^{-1}. The Raman spectra taken for MnTe films clearly show that in this range very high peaks of energy, corresponding to optical phonons in Te, can be found [3]. It is very probable that because of the presence of the phonon peak no two-magnon Raman scattering has been observed experimentally in MnTe films or bulk mixed crystals [3–5]. As a rule in antiferromagnetic systems two-magnon peaks are well defined and much easier to detect than those corresponding to one-magnon. However, it is also possible that very careful analysis of Raman intensity in the vicinity of the phonon Te peak could reveal a presence of the two-magnon peak.

5. Summary and conclusions

Self-consistent and uniform calculations of thermodynamic properties performed for MnTe systems within the framework of the Green's function formalism are presented. Using parameters known from the neutron diffraction studies, and fitting only the anisotropy constant, close consistency is obtained with Raman results for the temperature dependence of the spin-wave energy E_0, as well as for the integrated intensity. The anisotropy energy found in this paper is much smaller than the exchange energy, which is consistent with the conclusions drawn on the basis of neutron diffraction studies. On the other hand, the ratio of ω_A/ω_E, estimated within the framework of the molecular-field theory on the basis of data obtained from Raman spectra using previous approaches, is definitely too high. The

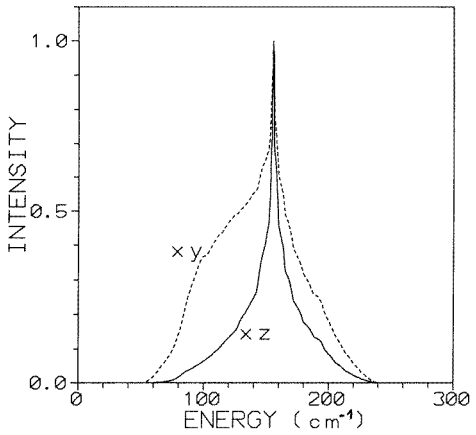

Figure 10. Two-magnon intensity as a function of energy.

exchange integrals deduced in such a way do not fit values known from other kinds of measurement [6–8, 11, 12].

Calculations performed in this paper also show that, in MnTe systems in a presence of the external magnetic field H_0, a separation of the modes E_0^+ and E_0^- can be smaller than $2g\mu_B H_0$. The result is confirmed by Raman data.

All the results show that the presented approach allows us to describe some properties of MnTe systems in a quite satisfactory way.

The studies performed in the paper clearly show that additional Raman investigations should be undertaken. Measurements in the external magnetic fields would be especially interesting.

Acknowledgments

The author is very indebted to Dr W Szuszkiewicz and Dr M Jouanne for the opportunity of using their experimental results prior to publication as well as to Professor J Barnaś for many helpful discussions and his critical reading of the manuscript. The work was supported by the Polish Research Committee, project no PB 750/T08/95/09.

References

[1] Giebułtowicz T M, Kłosowski P, Samarth V, Luo H, Furdyna J K and Ryhne J J 1993 *Phys. Rev.* B **48** 12 817

[2] Janik E, Dynowska E, Bąk-Misiuk J, Leszczyński M, Szuszkiewicz W, Wojtowicz T, Karczewski G, Zahrzewski A K and Kossut J 1995 *Thin Solid Films* **267** 74

[3] Szuszkiewicz W, Jouanne M, Dynowska E, Janik E, Karczewski G, Wojtowicz T and Kossut J 1995 *Acta Phys. Pol.* A **88** 941

[4] Szuszkiewicz W, Dynowska E, Janik E, Karczewski G, Wojtowicz T, Kossut J, Jouanne M and Gębicki W 1996 *23rd Int. Conf. on the Physics of Semiconductors (Berlin, 1996)* vol 1, ed M Scheffler and R Zimmermann (Singapore: World Scientific) p 385

[5] Venugopalan S, Petrou A, Gałazka R R and Ramdas A K 1981 *Solid State Commun.* **38** 365
Venugopalan S, Petrou A, Gałazka R R, Ramdas A K and Rodriguez S 1982 *Phys. Rev.* B **25** 2681
Petrou A, Peterson D L, Venugopalan S, Gałazka R R, Ramdas A K and Rodriguez S 1983 *Phys. Rev.* B **27** 3471

[6] Giebułtowicz T M, Rhyne J J, Ching W Y, Huber D L, Furdyna J K, Lebech B and Gałazka R R 1983 *Phys. Rev.* B **39** 6857
[7] Ching W Y, Huber D L and Leung K M 1980 *Phys. Rev.* B **21** 3708
[8] Ching W Y and Huber D L 1982 *Phys. Rev.* B **25** 5761
[9] Barnaś J and Świrkowicz R *Physica* B to be published
[10] ter Haar D and Lines M R 1962 *Phil. Trans.* A **255** 1
[11] Foner S, Shapira Y, Heiman D, Kershaw R, Dwight K and Wold A 1983 *Phys. Rev.* B **39** 11 793
[12] Wang X, Heiman D, Foner S and Becla P 1990 *Phys. Rev.* B **41** 1135
[13] Hewson A C and ter Haar D 1964 *Physica* **30** 890
[14] Lines M E 1964 *Phys. Rev.* **135** A1336
[15] Szuszkiewicz W, Jouanne M, Dynowska E, Janik E, Karczewski G, Wojtowicz T and Kossut J to be published
[16] Sawicki M, Kolśnik S, Wojtowicz T, Karczewski G, Janik E, Kutrowski M, Zakrzewski A, Dynowska E, Dietl T and Kossut J 1995 *Acta Phys. Pol.* A **87** 169
[17] Cottam M G 1975 *J. Phys. C: Solid State Phys.* **8** 1933
[18] Psaltakis G C and Cottam M G 1982 *J. Phys. C: Solid State Phys.* **15** 4847
[19] Callen H B and Strikman S 1965 *Solid State Commun.* **3** 5
[20] Elliot R J and Thorpe M F 1972 *J. Phys. C: Solid State Phys.* **5** 1461
[21] Balucani U and Tognetti V 1973 *Phys. Rev.* B **8** 4247